Steric Stabilization of Lipid/Polymer Particle Assemblies by Poly(ethylene glycol)-Lipids

Julie Thevenot,[†] Anne-Lise Troutier,[‡] Laurent David,[§] Thierry Delair,[†] and Catherine Ladavière*,[†]

UMR 2714/CNRS/bioMérieux, Systèmes Macromoléculaires et Physiopathologie Humaine, Ecole Normale Supérieure de Lyon, 46 Allée d'Italie, 69364 Lyon Cedex 07, France, Laboratoire des Matériaux Inorganiques, UMR 6002, Université Blaise Pascal, 24 Avenue des Landais, 63177 Aubière Cedex, France, and Laboratoire des Matériaux Polymères et Biomatériaux, UMR 5223 IMP, Université Lyon 1, Bât. ISTIL, 15 Bd Latarjet, 69621 Villeurbanne Cedex, France

Received July 9, 2007; Revised Manuscript Received August 22, 2007

Biocompatible and biodegradable assemblies consisting of spherical particles coated with lipid layers were prepared from sub-micrometer poly(lactic acid) particles and lipid mixtures composed of 1,2-dipalmitoyl-*sn*-glycero-3-phosphocholine and 1,2-dipalmitoyl-3-trimethylammonium-propane. These original colloidal assemblies, named LipoParticles, are of a great interest in biotechnology and biomedicine. Nevertheless, a major limitation of their use is their poor colloidal stability toward ionic strength. Indeed, electrostatic repulsions failed to stabilize LipoParticles in aqueous solutions containing more than 10 mM NaCl. By analogy with the extensive use of poly(ethylene glycol) (PEG)−lipid conjugates to improve the circulation lifetime of liposomes in vivo, 1,2-dipalmitoyl-*sn*-glycero-3-phosphoethanolamine-*N*-[methoxy(polyethylene glycol)] with various PEG chain lengths was added to the lipid formulation. Here, we show that LipoParticle stabilization was enhanced at least up to 150 mM NaCl (for more than 1 year at 4 °C). To determine the structure of PEG-modified LipoParticles as a function of the PEG chain length and the PEG-lipid fraction in the lipid formulation, a thorough physicochemical characterization was carried out by means of many techniques including quasi-elastic light scattering, zeta potential measurements, transmission electron microscopy, ^{1}H NMR spectroscopy, and small-angle X-ray scattering. Finally, an attempt was made to link the resulting structural data to the colloidal behavior of PEG-modified LipoParticles.

Introduction

LipoParticles are hybrid assemblies composed of a particle core surrounded by lipid layers.[1] These lipid/polymer particle assemblies are mainly involved in biotechnological and biomedical applications (in vitro[2−6] or in vivo[7−12]). The synthesis as well as an in-depth characterization of these species based on poly(styrene) particles and 1,2-dipalmitoyl-*sn*-glycero-3-phosphocholine (DPPC)/1,2-dipalmitoyl-3-trimethylammonium-propane (DPTAP) lipid mixtures were described in two previous papers.[13,14] However, for in vivo applications (e.g., in delivery applications of bioactive molecules or macromolecules), a biodegradable core would be more appropriate. Consequently, to go deeply into our investigation on LipoParticles, the previously used poly(styrene) particles were replaced by biodegradable poly(lactic acid) (PLA) ones with similar sizes (ca. 250 nm). The main drawback of LipoParticles highlighted for the first system (i.e., their poor stability with the increase in ionic strength of the continuous phase)[13,14] was found to be similar for the LipoParticles based on PLA particles. As shown in Table 1, the increase in ionic strength from 1 to 150 mM leads to a strong aggregation of LipoParticles by screening their electrostatic charges. This behavior would certainly be a limiting factor for their bioapplications.

Table 1. Mean Hydrodynamic Diameter (D_h), Size Distribution (POLY Value), and Zeta Potential (ζ) of Bare PLA Particles and LipoParticles (Synthesized in Water) Measured in 1−150 mM NaCl Solutions:

	D_h[b] (nm)	size distribution[c] (POLY value)	ζ (mV)
Bare PLA Particles[a]			
	247.5 ± 0.8	0.022 ± 0.005	− 70.1 ± 1.1
LipoParticles (DPPC/DPTAP 60/40 mol %)			
in 1 mM NaCl	277.4 ± 15.6	0.037 ± 0.018	+44.9 ± 3.3
in 10 mM NaCl	4690 ± 391	1[d]	ND[e]
in 150 mM NaCl	3732 ± 512	1[d]	ND[e]

[a] The D_h and POLY values of bare PLA particles remained constant at least up to 150 mM. [b] The standard deviations were obtained from three experiments. [c] See definition of POLY value in the Experimental Section. [d] A POLY value of 1 corresponds to the maximum one (experimentally measurable). [e] Not determined (due to strong aggregation).

To improve the LipoParticle colloidal stability, poly(ethylene glycol)−lipid (PEG-lipid) conjugates were incorporated in the lipid formulation because they drastically enhanced the stability of the liposomes in many recent applications. For instance, the in vivo circulation times of many drugs[15] (e.g., doxorubicin[16,17] or cisplatin[18,19]) encapsulated in PEG-grafted liposomes were significantly increased with an enhanced therapeutic effect and/or a reduced toxicity. Recently, antibodies modified with PEG-lipids were inserted in long-circulating PEG−liposomes.[20,21] In this system, PEG chains were not only used to sterically stabilize

* Author to whom correspondence should be addressed. E-mail: Catherine.Ladaviere@ens-lyon.fr.
[†] Ecole Normale Supérieure de Lyon.
[‡] Université Blaise Pascal.
[§] Université Lyon 1.

10.1021/bm700753q CCC: $37.00
Published on Web 10/25/2007

the assemblies but also as spacer arms to improve the accessibility of antibodies for the targeting of tumor cells. For transfection purposes or other therapeutic strategies involving nucleic acids, cationic liposomes incorporating PEG-lipids were applied as carriers of oligonucleotides[22] and plasmid DNA,[23] resulting in enhanced uptake by cells. Delivery of peptides (e.g., vasopressin)[24,25] and proteins (e.g., insulin)[26] was also described, the PEG chains providing an efficient protection for these molecules, which usually present a rapid clearance from the blood. Liposomes with grafted PEG were promising for vaccine development too, as proven with gp41 proteins of HIV-1.[27] Another striking innovative use of PEG-lipids was given by the modification of hemoglobin-encapsulating liposomes. They provided long-circulating red blood cell substitutes, having sufficient lifetime and hemoglobin content to be envisioned as artificial oxygen carriers.[28] Finally, another application of PEG-modified liposomes was in tumor diagnostics by positron emission tomography imaging.[29] To this end, small long-circulating liposomes encapsulating positron emitters were prepared. They were shown to avoid liver trapping and to accumulate in tumor tissues and so were revealed to be interesting tools for diagnostics by tumor imaging. In conclusion, by similitude to the above-demonstrated interests of PEG chains, the incorporation of PEG-lipids in the lipid formulation during the LipoParticle preparation was expected to improve the colloidal stability of the resulting assemblies. Besides, it is worth noting that, in the above-considered bioapplications, the lengths of the PEG chains played a significant role.[30] This length is controlled by the molecular weight choice of the carboxylic analogues of PEG polymers covalently attached onto the polar head group of phosphatidyethanolamine.[31] Consequently, in the study presented here, three commercial PEG_n−lipids, with three different chain lengths or molecular weights (with a degree of polymerization of $n = 16$, 45, or 113), were used to examine if in our case this parameter must also be taken into account.

The aim of this paper is to present the preparation and the characterization of PEG-modified LipoParticles in terms of (i) adsorption of PEG_n−lipids and DPPC/DPTAP lipids onto poly(lactic acid) particles, (ii) thickness of the resulting lipid layers, and (iii) spatial organization of PEG_n−lipids in lipid layers. These data are mainly provided by quasi-elastic light scattering (QELS), zeta potential measurements, transmission electron microscopy (TEM), ^{1}H NMR spectroscopy, and small-angle X-ray scattering (SAXS). This characterization provides a better understanding of the impact of the PEG_n−lipid incorporation in the lipid formulation on the colloidal stability of obtained LipoParticles. Hence, a correlation between the structural characteristics and the colloidal behavior of PEG-modified LipoParticles can be established.

Experimental Section

Materials. The zwitterionic lipid, DPPC, of the highest purity available was purchased from Sigma Chemical Co. (St. Louis, MO). The cationic lipid, DPTAP, and the PEG_n−lipids, 1,2-dipalmitoyl-*sn*-glycero-3-phosphoethanolamine-*N*-[methoxy(polyethylene glycol)] (PEG-PE), were obtained from Avanti Polar Lipids, Inc. (Alabaster, AL). According to the supplier, the molecular weights of PEG were 750, 2000, and 5000 g mol^{-1} (PEG_{16}-PE, PEG_{45}-PE, and PEG_{113}-PE, respectively). All lipids were used without further purification. Note that all lipids possess saturated fatty acids and the same carbon number in their hydrophobic tails, preventing phase segregation phenomena in the membrane. Racemic poly(D,L-lactic acid) (PLA_{50} with $M_n = 30\,000$ g mol^{-1}, molecular weight distribution $M_w/M_n = 1.7$) was purchased from Phusis (Grenoble, France) and used as received. Vesicles and LipoParticles were prepared either in distilled sterile water (Versol, Aguettant, Lyon, France) or in different saline solutions.

Preparation of PLA Particles. PLA nanoparticles were synthetized according to Fessi et al.[32] by the nanoprecipitation method. Briefly, the polymer was dissolved in acetone (a good solvent of the polymer) to reach a concentration of 20 g L^{-1}. This solution was then slowly added to an aqueous solution (a nonsolvent of the polymer) under moderate stirring. No surfactant was used. The solvent-to-dispersive phase volume ratio was $r = 1.5$. After the addition, the solvents were evaporated under vacuum at room temperature. The nanoparticle dispersions were stored in water at 4 °C and were stable for at least 6 months. The final polymer concentrations were between 20 and 50 g L^{-1} (depending on the particle batch). They were precisely measured by weighing of the wet and dried materials.

Vesicle Preparation. Lipids in desired proportions were dissolved in chloroform, and the solvent was then removed by rotary evaporation under reduced pressure, yielding a homogeneous and thin lipid film. Large multilamellar vesicles (LMVs) were obtained by adding distilled sterile water (to obtain a final lipid concentration of 10 mM) to the film and by stirring this mixture in a water bath at 70 °C. This temperature was chosen above the major phase transition temperature of main lipids, T_m, ($T_{m\,DPPC} = 41.4$ °C[33] and $T_{m\,DPTAP} = 49.3$ °C[34]). Smaller vesicles with a lower number of bilayers were prepared by disruption of the LMV suspension using a bath sonicator thermostated at 70 °C (Branson 3510, Branson Ultrasonics Co., Danbury, CT).

LipoParticle Synthesis. LipoParticles were prepared by adding the preformed vesicle dispersion to the PLA particles (with a final solid content of 0.2%). The driving forces leading to the LipoParticle formation were expected to be of an electrostatic nature (between anionic carboxylic charges of the PLA surface and cationic charges of the vesicles). The mixture was vortexed for 1 h at 70 °C (i.e., at $T > T_m$ to favor the lipid reorganization onto particles) at 1300 rpm. Thereafter, the dispersion was centrifuged at 4000*g* for 15 min at 15 °C to separate LipoParticles from non-adsorbed lipids. The pellet containing LipoParticles was redispersed in pure water. The supernatant was used to determine the free lipid concentration and consequently the amount of adsorbed lipids onto PLA particles. The DPPC concentration was determined by using a titration method based on enzymatic degradation[35] (PAP 150 kit, bioMérieux, Marcy-l'Etoile, France). In this method, phospholipids were hydrolyzed by phospholipase D, and the hydrogen peroxide (arising from oxidation of the liberated choline) was quantified. The equivalent number of lipid bilayers adsorbed onto the particles was calculated from the surfaces of the particles, the cross-sectional area of a DPPC molecule, the DPPC concentration, and the assumption that the adsorption of other lipids was proportional to their molar percentage in the initial lipid formulation. Note that this assumption was generally valid in our cases because the lipids were initially introduced in large excess; the error in the determination of the equivalent number of adsorbed bilayer was consequently lower than 5%.

LipoParticles were always prepared with an excess of vesicles compared to particles. This excess (defined by surface area considerations, expressed by the specific notation A_v/A_p and well-described in previous papers)[13,14] was equal to 14 for all experiments, corresponding to a final lipid concentration of 2.6 mM before centrifugation (except for NMR analyses where $A_v/A_p = 3$).

Note that all of the below-described analyses (QELS, zeta potential measurement, NMR, SAXS, and microscopy techniques) were performed on LipoParticles free of non-adsorbed lipids (i.e., after centrifugation steps). Concerning the study about the effect of ionic strength on the LipoParticle colloidal stability, it was carried out after an additional centrifugation step followed by a redispersion of the obtained pellet in a medium of the desired ionic strength.

Quasi-Elastic Light Scattering. Mean hydrodynamic diameters (D_h) and mean size distributions (POLY) were determined at 25 °C by QELS (Zetasizer 3000 HS, Malvern Instruments, U. K.). The measurement angle was 90°, the laser was a He−Ne type operating at 633 nm, and

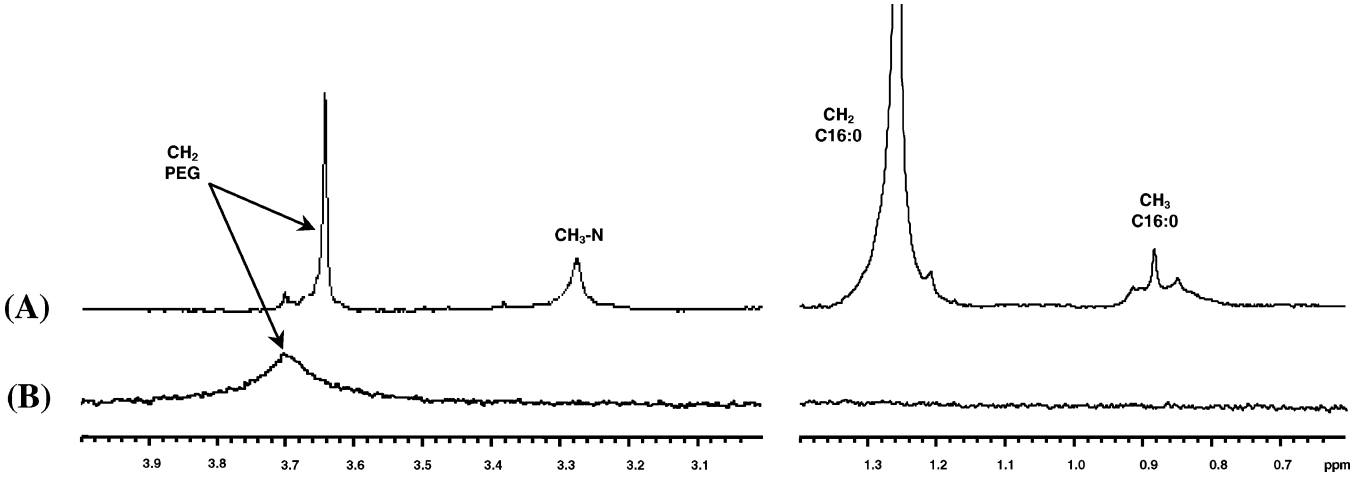

Figure 1. ^{1}H NMR spectra used to determine (A) the quantity of adsorbed lipids (25 °C, LipoParticles dried and dissolved in $CDCl_3$) and (B) the mobility of adsorbed lipids (25 °C, colloidal dispersion of LipoParticles in D_2O).

the solvent refractive index and viscosity at 25 °C were 1.33 and 0.8904 cP, respectively. The POLY value (ranging from 0 to 1) is a dimensionless measure of the distribution broadness (defined by $\mu_2/\langle\Gamma\rangle^2$, where μ_2 is the second cumulant of a correlation function analyzed by the cumulant method[36] and $\langle\Gamma\rangle$ is the average decay rate). For a monodisperse sample, the POLY value should theoretically be zero. In practice, a POLY value for a "monodisperse" latex lies between 0 and 0.05.[37] The polydispersity can be considered to have lost its significance for values above 0.15, but below a value of 0.5 useful comparison between samples can be made. Samples were diluted in a 1 mM NaCl solution before measuring the intensities of autocorrelation functions. Typically, five independent measurements were recorded to obtain a mean hydrodynamic diameter and a mean POLY value.

Electrophoretic Mobility Measurements. The electrophoretic mobility values were measured at 25 °C using a Zetasizer 3000 HS apparatus (Malvern Instruments, U. K.). Electrophoretic mobility (μ_e) was converted to zeta potential (ζ) according to Smoluchowski's equation (eq 1)[38]

$$\mu_e = \frac{\epsilon_o \epsilon_r}{\eta} \zeta \tag{1}$$

where η, ϵ_o, and ϵ_r are the medium viscosity, permittivity of vacuum, and relative permittivity, respectively. Samples were diluted in a 1 mM NaCl solution, and five independent measurements were recorded to obtain a mean zeta potential value.

Transmission Electron Microscopy. TEM observations were performed on a CM 120 Philips electron microscope at an accelerating voltage of 80 kV (at CTμ, Claude Bernard University, Lyon, France). Samples were deposited on carbon/Formvar-coated copper grids (Spi Supplies, Structure Probe Inc., West Chester, PA) and stained with sodium silico tungstate (1% w/v) purchased from Sigma Chemical Co. (St. Louis, MO).

^{1}H NMR. ^{1}H NMR experiments were performed on LipoParticles either dried and then dissolved in deuterated chloroform ($CDCl_3$, 99.80%, 1% tetramethylsilane, SDS, Peypin, France) or in a dispersion in deuterated water (D_2O, 99.90%, SDS, Peypin, France). The lipid concentration in LipoParticle samples was ca. 1 g L^{-1}. ^{1}H NMR spectra were recorded using a 200 MHz spectrometer (Bruker AC200). Dimethylformamide (DMF; Sigma Chemical Co., St. Louis, MO) in $CDCl_3$, or deuterated trimethylsilyl-3-propionic acid (d_4-TMSP, SDS, Peypin, France) in deuterated water were used as internal references for chemical shifts and/or quantification.

^{1}H NMR spectra of PEG-modified LipoParticle dispersions measured in deuterated water enabled us to quantify, by using a d_4-TMSP internal standard signal, the PEG chains located on the LipoParticle surface. Indeed, NMR spectra of PEG−LipoParticles in D_2O (see example in Figure 1B) only showed the resonance of methylene protons of external PEG chains in the 3.5−3.9 ppm region (given that the other constituents of the LipoParticles are in a "solid-like" state, see definition in the Results and Discussion section). The number of protons corresponding to this region was calculated according to Vernooij et al.[39] Then, the distance between grafting points of PEG chains on the LipoParticle surface, D, was calculated from the mean area available for one PEG chain, *A* (determined by taking into account the LipoParticle surface area estimated by QELS data[40] and the total quantity of PEG chains in the outer monolayer detected by ^{1}H NMR), and the assumption that the PEG chain repartition on the LipoParticle surface was a plane centered hexagonal lattice

$$D = 2\sqrt{\frac{\sqrt{3}A}{6}} \tag{2}$$

For the quantification of the total amount of lipid in LipoParticles, the same samples were dried under vaccum and completely dissolved in $CDCl_3$. This amount was expressed as the equivalent number of bilayers on the surfaces of PLA particles.[13] This number was calculated by using the integrals of $-C\mathbf{H_3}$ and $-C\mathbf{H_2}-$ peaks of the fatty acid parts of the lipids (Figure 1A; $\delta = 0.88$ for I_{CH_3} and 1.26 ppm for I_{CH_2}, respectively), the integral of the $-C\mathbf{H}-$ peak from PLA ($\delta = 5.0-5.4$ ppm), and the following equation

$$\text{equivalent number of bilayers} = \frac{\sigma_{lipid}\rho_{PLA}R_{PLA}N}{6\times 10^{21}} \times \frac{\frac{1}{2}\left(\frac{I_{CH_3}}{6}+\frac{I_{CH_2}}{48}\right)_{lipid}}{M_{PLA}\left(\frac{I_{CH}}{1}\right)_{PLA}} \tag{3}$$

with σ_{lipid}, the mean area occupied by the DPPC polar head (0.7 nm^2 at $T > T_m$),[41] ρ_{PLA}, the PLA density (i.e., $\rho_{PLA} \approx 1.25$),[42] *N*, Avogadro's number, *R*, the mean radius of PLA particles in nanometers (from QELS data), M_{PLA}, the molecular weight of the PLA repeat unit (72 g mol^{-1}), and I_{CH_i}, the considered proton integrals measured by ^{1}H NMR. The total amount of PEG-lipids in LipoParticle samples was quantified by using the integral of the methylene protons of PEG chains (all PEG protons resonating because samples were perfectly solubilized in $CDCl_3$). As shown in the spectrum of Figure 1A, the chemical shift of the PEG methylenes (corresponding to 62, 178, or 450 protons for $n = 16$, 45, or 113, respectively)[39] was 3.64 ppm in $CDCl_3$.

Small-Angle X-ray Scattering. SAXS measurements were carried out at the BM2 (D2AM French CRG Beamline) of the European Synchrotron Radiation Facility (ESRF, Grenoble, France) working at ~200 mA. The wavelength of the incident beam was set to $\lambda = 0.81606$ Å (corresponding to an incident photon energy of $E = 15$ keV). The

Scheme 1. (A) Chemical Formulas of PEG_n−Lipids (1,2-Dipalmitoyl-*sn*-glycero-3-phosphoethanolamine-*N*-[methoxy-(polyethylene glycol)]) and (B) Three-Dimensional Models (Space Filling without Molecular Dynamics Calculations) of PEG_n−Lipids with Different PEG Chain Lengths (n = 16, 45, or 113)

(A) Chemical formula of PEG_n-lipids

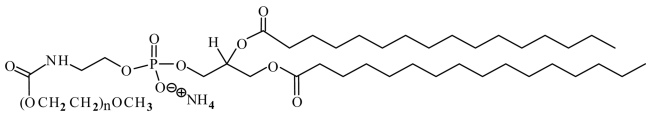

(B) 3-D models of PEG_n-lipids

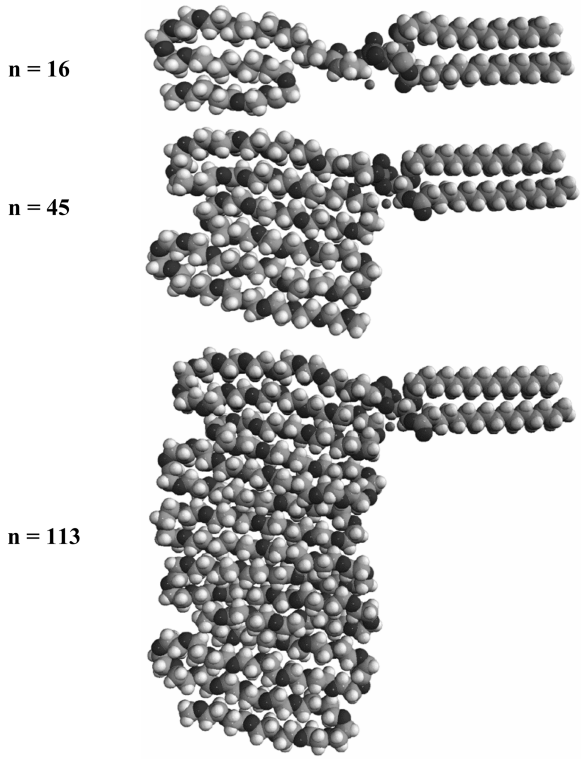

samples (dispersions with concentrations from 100 to 200 g L^{-1}) were placed in glass capillaries with internal diameters of 1.5 mm, thermostated at 25 °C. A two-dimensional charge coupled device (CCD) detector (Ropper Scientific) was used and placed at ~35 cm from the samples with an exposure time close to 0.5 s for all samples (including the empty cell measurements and dark images). Silver behenate was used for the q-range calibration (where q is the scattering vector defined as $q = 4\pi \sin(\theta)/\lambda$). The scattered images were corrected for the individual sensitivity of each pixel and the dark current signal as well as for the glass capillary and other windows response (subtraction of the scattered data from capillaries filled with solvent). The distortion introduced by the taper of the detector was also corrected. Finally, the radial averages around the image center (weighted center of the incident beam) were calculated. These numerical computations were performed by a software developed and provided on the beamline (BM2IMG).

Considering the size of the LipoParticles, the SAXS experiments were carried out in Porod's domain ($1 < qR_g$, where R_g is the particle gyration radius). The q-range available was $0.01 < q < 0.3$ Å^{-1}. In terms of electron density, the lipid layer constituted a transition layer between the PLA particle and the liquid phase. This transition layer can be detected by SAXS when the slope α of the $\log(I(q))$ vs $\log(q)$ plot is slightly higher than 4 (this value corresponding to the theoretical case of a sharp variation of scattering power across the interface of the particles). In the case of a transition layer, Porod's law can be modified by the introduction of an additional term scaling as $1/q^2$ yielding

$$I(q) = \frac{C}{q^4} - \frac{B}{q^2} \tag{4}$$

which enables the determination of the width of the transition layer. The electron density profile of the transition layer was considered to be linear,[43] and its thickness (Li) could be determined from the value of Porod's constant, C, the value of B deduced from the linear regression plot of $I(q)q^2$ versus $1/q^2$, and $\mathrm{Li} = \sqrt{12\pi B/C}$.

Results and Discussion

The association of polymer particles with preformed vesicles can lead to original assemblies named LipoParticles (as previously described).[13,14] To improve their colloidal stability, PEG chains were tethered on their surfaces thanks to the incorporation of PEG_n−lipids (with n = 16, 45, and 113) in the lipid formulation of vesicles. As in the liposome case, the colloidal stability is indeed expected to be promoted by PEG chain steric repulsions and, according to Tirosh et al.,[44] by a decrease in bilayer defects due to a dehydration of the lipid headgroup region caused by strong hydration of the outer PEG layer. As shown in Scheme 1, the PEG conjugates used possess saturated fatty acids and the same carbon number in their hydrophobic tails (i.e., C 16:0) as the two other lipids (zwitterionic DPPC and cationic DPTAP) composing the vesicle formulation. Steps leading to PEG-modified LipoParticles from PLA particles and PEG_n−lipid/DPPC/DPTAP vesicles are depicted in Figure 2 and detailed in the Experimental Section. With the aim of examining scrupulously the impact of PEG chains on the LipoParticle colloidal stability, the first syntheses were carried out with increasing the ionic strength of the medium during the LipoParticle preparation. With this process, high amounts of lipids were assayed for LipoParticles (Table 2), probably because of the screening effect of vesicle electrostatic charges leading to a lipid multilayer adsorption (black circles in Figure 3) as well as to vesicle adsorption without spreading onto particles (black arrows in Figure 3). As a result of these first observations, we chose (i) to synthesize PEG-modified LipoParticles in water (leading to PLA particles coated by a lipid bilayer and narrow size distributions of the resulting assemblies), (ii) to purify them by centrifugation steps, and (iii) to redisperse subsequently them in a medium of the desired ionic strength.

Physicochemical Investigation of the PEG-Modified Lipid Layers Surrounding Particles. A thorough physicochemical investigation of the PEG-modified lipid layers surrounding PLA particles was necessary to assess the impact of PEG chains on the colloidal stability of LipoParticles. Parameters such as the PEG_n−lipid amount actually adsorbed onto the PLA particles, the thickness of the adsorbed shell, and the location of the PEG_n−lipids (i.e., in external or internal monolayers) in the lipid bilayer were needed for a structural description of PEG-modified LipoParticles. This characterization was undertaken by ^{1}H NMR and SAXS analyses.

Quantification of PEG_n−Lipids Adsorbed onto Polymer Particles. The initial molar percentage of PEG_n−lipids in the vesicle formulation was 10% (completed with 50% DPTAP and 40% DPPC). But this initial percentage could actually be different in the lipid layers adsorbed onto polymer particles, because a vesicle excess (in surface area terms) with regard to particles was used and because a lipid reorganization occurred during the adsorption of vesicles.[45] Consequently, the amount of PEG_n−lipids really adsorbed onto particles was first scrutinized (as a function of PEG chain length). It was preliminarily checked that the total lipid quantity adsorbed onto particles,

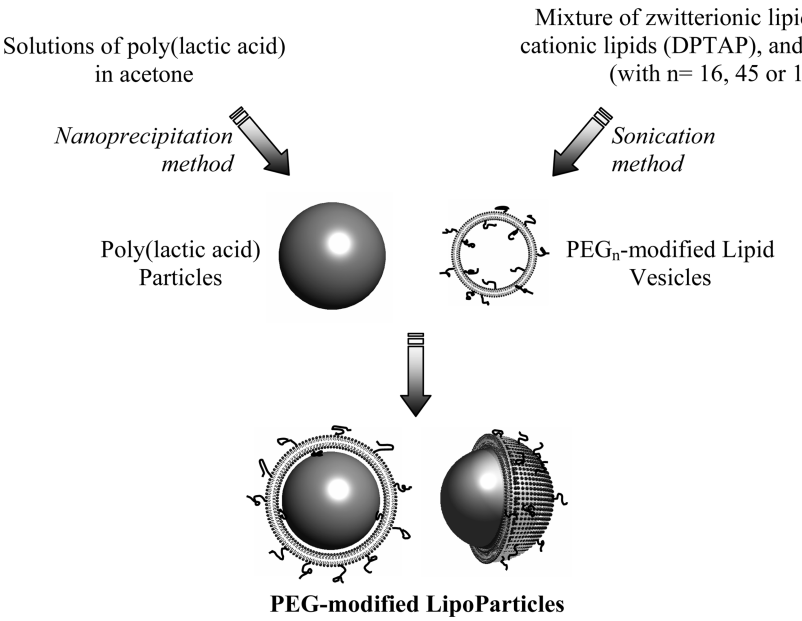

Figure 2. Schematic representation of the steps involved in PEG_n-modified LipoParticle synthesis.

Table 2. Equivalent Number of Lipid Bilayers Adsorbed onto Particles in Various Formulations of LipoParticles Synthesized in Media with Different Ionic Strengths

	equivalent number of lipid bilayers adsorbed[a]		
[NaCl] (mM)	DPPC/DPTAP (50/50 mol %)	PEG_{16}−lipid/ DPPC/DPTAP (10/40/50 mol %)	PEG_{45}−lipid/ DPPC/DPTAP (10/40/50 mol %)
0	1.3	1.2	1.0
10	1.8	2.2	1.4
50	3.9	3.9	1.4
100	3.3	4.2	2.1
150	5.3	5.9	2.6

[a] Determined by chemical assay (kit PAP 150, see Experimental Section).

determined by ^{1}H NMR spectroscopy (see calculations in the Experimental Section and spectrum in Figure 1A), corresponded to about one bilayer (second line, Table 3). Concerning the PEG_n−lipid adsorption, the molar percentage of PEG_n−lipids in the adsorbed lipid layer (below ca. 3%, third line in Table 3) differed from the molar percentage of PEG_n−lipids in initial vesicle formulation (i.e., 10%). Note that the data were similar when n was equal to 16 and 45 and even smaller for $n = 113$. The increase in PEG chain length would make the reorganization of PEG-modified vesicle onto particles more difficult.

Then, the influence of the molar percentage of PEG_n−lipids ($n = 45$) in the initial lipid formulation was studied. It showed that (i) the total lipid quantity adsorbed onto particles remained equal to one bilayer for all tested molar percentages (second line, Table 4), (ii) the relative PEG_{45}−lipid adsorption onto particles decreased with the increase in the amount of PEG_{45}−lipid initially inserted in the vesicles (third line compared to first one in Table 4), and (iii) a saturation level of adsorbed PEG_{45}−lipids (corresponding to ca. 3% of PEG_{45}−lipids in the coated lipid bilayer) was reached for an initial formulation containing 10% PEG_{45}−lipids. This limited adsorption could be explained by steric hindrance between PEG_{45} chains located at the surface of the adsorbed bilayer.

Organization of PEG_n−Lipids in the Lipid Layers Adsorbed onto Particle Surfaces. After the determination of the amount of PEG_n−lipids in the lipid bilayer, it was important to know their location within this bilayer. To obtain such information, we used NMR spectroscopy, which detects only the "mobile" species in the continuous phase of dispersions. In our systems, the polymer particles and lipid bilayers adsorbed onto particles cannot be detected in classical NMR experiments owing to their too long relaxation times. It was indeed verified that the DPPC/DPTAP lipids were not detected at 50 °C when they were adsorbed onto particles (due to strong lipid/particle interactions), whereas they were "visible" in the corresponding vesicles at the same temperature. Consequently, the mobile species in our systems only corresponded to water-soluble PEG chains expanded in an aqueous medium (i.e., PEG_n−lipids positioned in the outer monolayer). On the contrary, the PEG chains facing particles (i.e., PEG_n−lipids positioned in the inner monolayer) were expected to be nonmobile to a certain extent and thus not detectable in NMR experiments. In PEG-modified vesicles all of the PEG_n−lipid could be detected by NMR spectroscopy; thus there was no difference according to the location (in the inner or outer monolayer) in this case. Regarding PEG-modified LipoParticles, results in Table 3 (fourth line) show that ca. 50% of PEG_{16} chains were mobile. This demonstrated that the amount of PEG chains in the outer monolayer was the same as that in the inner one, and so an equal repartition was respected without a particular PEG_n−lipid redistribution during and after (by flip-flop exchange) bilayer formation. The molar percentage of mobile PEG chains increased with polymer length, meaning that the quantity of PEG_n−lipids in the inner layer decreased, probably because of the steric hindrance of long chains facing particles. For instance, only 10% of PEG chains of PEG_{113}−lipids were in the inner monolayer of PEG-modified LipoParticles. The exchange of PEG_{113}−lipids by trans-bilayer flip-flop between both monolayers did subsequently not occur. As already suggested by De Cuyper et al.[46,47] for PEG_n−lipid adsorption onto the surfaces of iron oxide cores,[48−50] these lipids are too bulky to pass through the hydrophobic zone of the bilayer.

Thickness of the Resulting Lipid Shell. Thereafter, the thickness of the PEG-modified lipid layer adsorbed onto PLA particles was assessed by SAXS analysis. In the case of LipoParticles, the electron density of PLA particles being different from the lipid layer one, the thickness of the adsorbed shell could be determined from calculations of transition layer

Table 3. Equivalent Number of Lipid Bilayers, Molar Percentages of PEG_n−Lipids and of Mobile PEG Chains Adsorbed onto Polymer Particles as a Function of PEG Chain Length (n)[a]

PEG chain length	$n = 16$	$n = 45$	$n = 113$
equivalent number of lipid bilayers adsorbed[b]	0.9 ± 0.2	0.9 ± 0.1	0.8 ± 0.1
PEG_n−lipids in the adsorbed lipid bilayer[c] (mol %)	2.7 ± 0.5	3.2 ± 0.5	1.9 ± 0.2
mobile PEG_n chains in the adsorbed lipid bilayer[c] (mol %)	52 ± 2	69 ± 7	90 ± 2

[a] The initial lipid formulation was PEG_n−lipid/DPPC/DPTAP (10/40/50 mol %). [b] Number calculated from the average of fatty acid $-CH_2-$ and $-CH_3$ integrals obtained by ^1H NMR (see Experimental Section). The standard deviations were obtained from three experiments with three different batches of PLA particles. [c] Quantification carried out from the PEG chain $-CH_2-$ integral measured by ^1H NMR (see Experimental Section). The standard deviations were obtained from three experiments with three different batches of PLA particles.

Table 4. Equivalent Number of Lipid Bilayers and Molar Percentage of PEG_{45}−Lipids in the Lipid Formulation of the Adsorbed Lipid Bilayer as a Function of PEG_{45}−Lipid Molar Percentage in the Initial Lipid Formulation

PEG_{45}−lipids in the initial lipid formulation (mol %)	1%	5%	10%	15%
equivalent number of lipid bilayers adsorbed[a]	1.0	1.1	0.9	0.9
PEG_{45}−lipids in the formulation of the adsorbed lipid bilayer[b] (mol %)	1.0	2.5	3.2	3.0

[a] Number calculated from the average of fatty acid $-CH_2-$ and $-CH_3$ integrals obtained by ^1H NMR. [b] Quantification carried out from the PEG chain $-CH_2-$ integral measured by ^1H NMR. Measurement error and accuracy: 1% and ±0.1 bilayer.

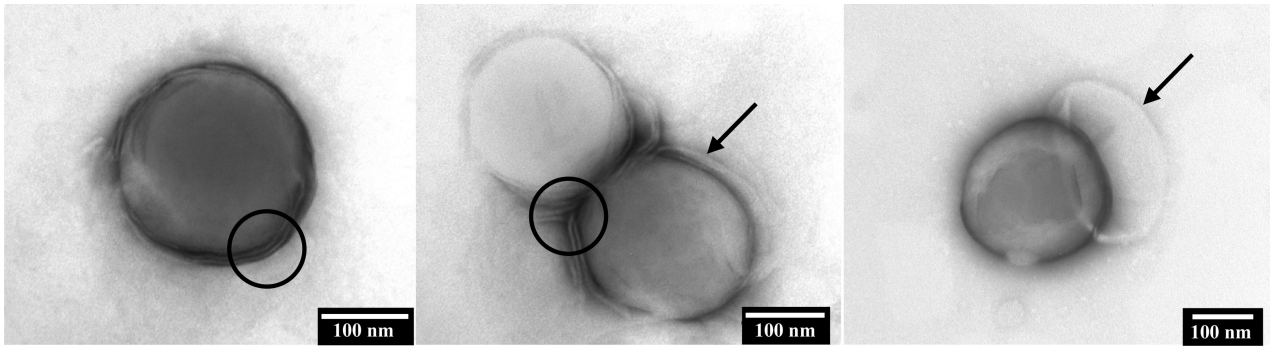

Figure 3. LipoParticles (PEG_{45}−lipid/DPPC/DPTAP 10/40/50 mol %) synthesized in 150 mM NaCl and observed by TEM after staining with sodium silico tungstate (1% w/v in water). Black circles and arrows indicate the lipid multilayers and vesicles adsorbed without spreading onto particles, respectively, correlating with the high lipid amount of 2.6 lipid bilayers presented in Table 2 at 150 mM NaCl.

Table 5. Thickness of the Transition Layer (Li) and Zeta Potential (ζ) of Bare PLA Particles, LipoParticles, and PEG-Modified LipoParticles in Water, as a Function of Chain Length (n), and Molar Percentage of PEG_{45}-Modified LipoParticles

		Li[c] (Å)	ζ (mV)
bare PLA particles[a]			−70.1
LipoParticles[b] (DPPC/DPTAP 60/40 mol %)		43	+44.9
PEG_n-modified LipoParticles (PEG_n−lipid/DPPC/DPTAP 10/40/50 mol %)	$n = 16$	67	+51.2
	$n = 45$	79	+25.7
	$n = 113$	98	+22.5
PEG_{45}-modified LipoParticles (PEG_{45}−lipid/DPPC/DPTAP x/50/(50 − x) mol %)	$x = 1\%$	52	+47.2
	$x = 5\%$	64	+36.7
	$x = 10\%$	79	+25.7

[a] For the bare polymer particles, no transition layer was observed. [b] Note that the lipid formulation for the reference non-PEG-modified LipoParticles was chosen in respect with global charge. [c] Measurement error: 10 Å.

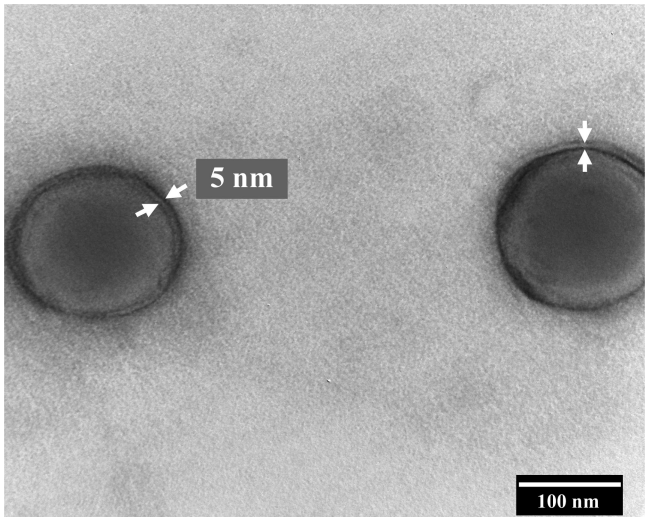

Figure 4. LipoParticles (PEG_{45}−lipid/DPPC/DPTAP 10/40/50 mol %) synthesized in pure water and observed by TEM after staining with sodium silico tungstate (1% w/v in water). White arrows indicate the lipid bilayer thickness measured from AnalySIS software (average determined with 30 measurements on 10 particles).

width (Li, see Experimental Section). The value of 43 Å (Table 5) obtained for lipid layer thickness in non-PEG-modified LipoParticles was consistent with that expected for a lipid bilayer (~5 nm).[41] This lipid bilayer can also be discerned in the TEM image (Figure 4) for LipoParticles with PEG_{45}−lipids. According to Table 5, the incorporation of PEG_n−lipids in the lipid formulation resulted in an increase in transition layer thickness, and more precisely, it linearly increased with the length of the PEG chains. It will be very interesting in the second part of this article to link this PEG length dependence of shell thickness to the study of the colloidal stability of the resulting LipoParticles.

The thickness of the PEG-modified lipid shell was also examined as a function of the molar percentage of PEG_{45}−lipids in the initial lipid formulation. Table 5 shows that this parameter had a direct effect on the transition layer; the higher

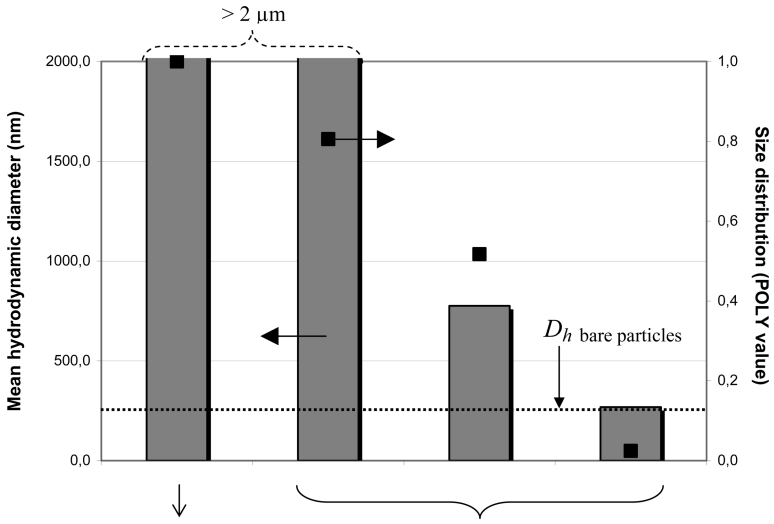

		PEG_{16}-lipid	PEG_{45}-lipid	PEG_{113}-lipid
Size Standard Deviation (nm)	iv	iv	360	1,4
POLY Standard Deviation	iv	0,335	0,134	0,003

Figure 5. Effect of the incorporation of PEG$_n$−lipids (with different chain lengths, PEG$_n$−lipid/DPPC/DPTAP 10/40/50 mol %) in lipid formulation on the mean hydrodynamic diameters and size distributions of the resulting species in comparison with LipoParticles (DPPC/DPTAP 60/40 mol %): left axis, diagrams; right axis, solid square. All samples were prepared in water and diluted in 150 mM NaCl (measurements 1 h after dilution, 25 °C). Standard deviations were calculated from at least three experiments with same batch of PLA particles. Here, iv represents incorrect values, i.e., results without scientific meaning (due to aggregation phenomena).

the molar percentage, the larger the thickness. This impact is already well-known for the PEG-modified liposomes, as a result of a modification of PEG chain conformation on the liposome surface with an increase in PEG$_n$−lipid molar precentage.[51] Indeed, the conformational change was described as a transition from a mushroom-like conformation at small PEG$_n$−lipid percentages to a brush-like (more expanded in the aqueous phase) at high percentages due to steric repulsions between PEG chains.

Finally, the comparison of these thicknesses with zeta potentials (Table 5) revealed that the higher values of thickness led to more important charge screening effects due to a shift of the shearing plane (where the measurement occurred) away from the particle surface. In fact, the absolute value of the zeta potential decreased with the length of PEG chains and their expansion in aqueous solution. A zeta potential decrease was also observed with the increase of the PEG$_{45}$−lipid molar percentage. This behavior cannot be attributed to the addition of anionic species (PEG$_{45}$−lipid) in the lipid formulation because the difference between $x = 1\%$ and 10% (corresponding to a real variation from 1% to 3% in the adsorbed lipid bilayer, Table 4) cannot explain such a change in zeta potential (ca. −20 mV). This change was rather due to the thickness dependence and the shielding effect, as discussed above.

Colloidal Stability of PEG-Modified LipoParticles toward Ionic Strength. The aim of the above physicochemical characterization of the particle coating by PEG-modified lipid layers was to contribute to a better understanding of the main features highlighted in the below LipoParticle colloidal stability study. This colloidal stability was investigated by diluting PEG-modified LipoParticles in media with growing ionic strength and by measuring the size parameters (mean hydrodynamic diameter and size distribution by QELS) of assemblies after this dilution step (incubation for 1 h at 25 °C with a solid content of 0.2%). The influence of the lengths as well as the molar percentages of PEG chains in the lipid formulations were considered.

Figure 5 exhibits the impact of the incorporation of PEG$_n$−lipids in lipid formulation as well as of the PEG chain length on the structural organization of the resulting LipoParticles in 150 mM NaCl. At this ionic strength, the assemblies without PEG$_n$−lipid were aggregated (as indicated by a very high mean hydrodynamic diameter and a broad size distribution). The incorporation of 10 mol % PEG$_{16}$−lipids in the lipid formulation did not provide any improvement in colloidal stability. The PEG$_{16}$ shell around LipoParticles (67 − 43 = 24 Å, Table 5) would not be sufficient to induce efficient steric stabilization of LipoParticle assemblies. Note that the value of the zeta potential was not affected either by the PEG$_{16}$ shell at this molar percentage (i.e., 10 mol %) contrary to the other PEG formulations (Table 5). In this case, the PEG$_{16}$ shell was probably too thin to screen the lipid charge. The insertion of PEG$_n$−lipids with higher n values in the lipid formulation improved the colloidal stability, as pointed out by the obvious decreases in mean hydrodynamic diameter and size distribution. Moreover, the decrease in standard deviations demonstrated that the results became more and more reproducible with PEG chains of increasing lengths, i.e., with increasing effectiveness of steric stabilization by PEG chains. Nevertheless, the size parameters of PEG$_{45}$-modified LipoParticles remained affected by 150 mM NaCl, as shown in Figure 6 (i.e., individualized assemblies were obtained in water whereas large aggregates were observed in 150 mM NaCl solution). Concerning the size and size distribution of PEG$_{113}$-modified LipoParticles, they were very reproducible (low standard deviations), and their characteristics were close to those of non-PEG-modified LipoParticles in water. In this case, the shell thickness measured by SAXS was 98 Å (Table 5), which corresponded to a difference of 55 Å compared to non-PEG-modified LipoParticles. This additional PEG shell would ensure sufficient steric repulsion between modified LipoParticles. It is worth noting that the colloidal stability could not be explained by a higher fraction of PEG chains located in

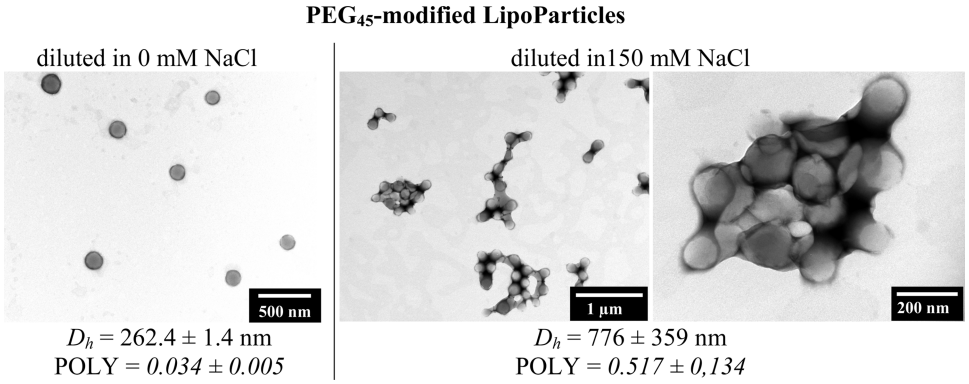

Figure 6. TEM micrographs (samples stained with sodium silico tungstate 1% w/v in water), mean hydrodynamic diameter (D_h), and POLY values (determined by QELS) of LipoParticles modified with 10 mol % PEG_{45}−lipid (PEG_{45}−lipid/DPPC/DPTAP 10/40/50 mol %, after incubation in 0 or 150 mM NaCl). Note that the staining appears to be positive in this case maybe due to the surface charges of LipoParticles.

Table 6. Distance between PEG Grafting Points (D), Physical Size of Polymer Chain in a Good Solvent (R_F), and Conformation of the Grafted Polymer Depending on D and R_F

	D^a (nm)	$R_F{}^b$ (nm)	conformation of grafted polymer[c]
PEG_{16}−lipid/DPTAP/DPPC (10/40/50 mol %)	5.4	1.9	distant mushrooms
PEG_{45}−lipid/DPTAP/DPPC (10/40/50 mol %)	4.3	3.4	mushroom
PEG_{113}−lipid/DPTAP/DPPC (10/40/50 mol %)	4.9	6.0	brush

[a] See calculations in the Experimental Section. [b] $R_F = an^{3/5}$ with a being the monomer size (0.35 nm for PEG)[52] and n being the degree of polymerization.[53] [c] Three regimes of grafted polymer behavior depending on D: $D > 2R_F$ (distant mushrooms, i.e., mushrooms that can interdigitate when two PEG-covered surfaces are in close proximity), $2R_F > D > R_F$ (mushroom), $D < R_F$ (brush).[55]

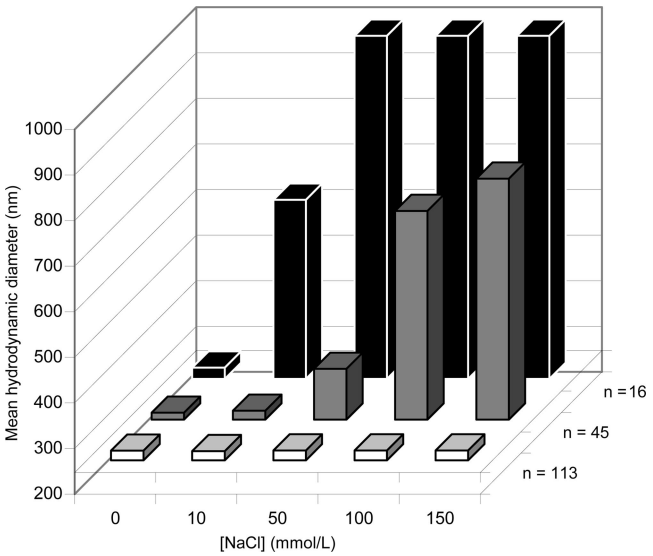

Figure 7. Influence of both PEG chain length (5 mol % in the lipid formulation) and ionic strength (i.e., NaCl concentration) on LipoParticle colloidal stability (1 h at 25 °C). The floor (*xy* plane) corresponds to the hydrodynamic diameter of the bare PLA particles.

the outer monolayer (which increased with n, Table 3) because the amount of total PEG chains in the outer monolayer was equivalent for $n = 45$ ($0.69 \times 3.2 = 2.2\%$, Table 3) and 113 ($0.90 \times 1.9 = 1.7\%$, Table 3). As a result, the distinction in colloidal behavior could rather be attributed to a conformation difference (mushroom-like or brush-like for PEG_{45}- or PEG_{113}-modified LipoParticles, respectively), as determined from the distance D (distance between PEG chain grafting points, see calculations in the Experimental Section) and discussed below.

Indeed, the quantification of the externally located PEG chains by NMR allowed us to estimate distance D for each PEG chain length (Table 6). This distance was then compared to the physical size of the polymer chain coil in a good solvent (Flory radius, $R_F = an^{3/5}$ with n being the degree of polymerization and a being the monomer size, i.e., 0.35 nm for PEG[52]).[53] According to the literature,[52,54,55] the conformation of the PEG chains within the polymer layer tethered onto a liposome surface is brush-like if $D < R_F$, mushroom-like if $2R_F > D > R_F$, and distant mushroom-like if $D > 2R_F$. According to Table 6, brush conformation is expected for PEG_{113}-modified LipoParticles, mushroom conformation for PEG_{45} ones, and distant mushroom conformation for PEG_{16} ones.

The distance D can also be used to forecast the PEG layer thickness. Indeed, for the PEG chains in the mushroom regime, the thickness of the polymer layer is assumed to be equal to R_F.[53] For PEG_{45}-modified LipoParticles, R_F was found to be 3.4 nm, that is to say a resulting shell of LipoParticles of 7.7 nm (Table 5) in comparison with a transition layer of 7.9 nm directly determined from SAXS data (Table 5). Concerning the brush regime, due to lateral interactions between the polymer chains, the extension of the chains is assessed from the following equation[53]

$$L_{\text{brush}} = \frac{na^{5/3}}{D^{2/3}} \quad (5)$$

with L_{brush} being the thickness of the polymer layer in the brush regime, n being the degree of polymerization, and a being the monomer size (0.35 nm for PEG[52]). Hence, for LipoParticles prepared with 10 mol % PEG_{113}−lipid, L_{brush} was equal to 6.8 nm, corresponding to a resulting shell thickness of 11.1 nm, which had to be compared with a transition layer of 9.8 nm measured by SAXS (Table 5). Thus, the experimental thicknesses determined by SAXS were in rather good correlation with these theoretical estimations. Consequently, in the case of LipoParticles, the mushroom/brush formalism can be used to predict the stability of systems (as well as in the liposome case).

Still concerning the study of the influence of PEG chain length, Figure 7 displays the critical ionic strength value from which the PEG_n-modified LipoParticles became aggregated systems. This ionic strength was 10 mM with PEG_{16}−lipids,

50 mM with PEG_{45}−lipids, and did not exist at least up to 150 mM with PEG_{113}−lipids. To conclude, the longest PEG chains provided the best colloidal stability because the corresponding LipoParticle shell was the thickest, and thus, steric repulsions between assemblies were the most efficient. Note that this explanation assumes that the trend observed in water (i.e., the higher the *n* value, the larger the transition layer) remains the same at different ionic strengths.

The characterization of PEG_n-modified LipoParticles and, particularly, the determination of the amount of PEG_n−lipids really adsorbed onto particles (as described in the physicochemical investigation part) revealed that this quantity was very low compared to the initial input. Despite this, we carried out a study on the influence of the molar percentage of PEG_n−lipids in the initial lipid formulation on the colloidal stability of the assemblies (Figure 8). The macroaggregation, annotated on the graphs (solid ellipsoidal lines), corresponded to an irreversible coagulation that was visible in the samples by a phase separation. This macroaggregation phenomenon was less marked when the PEG chain length increased. For example, in the PEG_{113}−lipid case, only the formulations with low amounts of modified lipids (1 mol %) were not stable. For the other molar percentages and for all of the studied NaCl concentrations, the assemblies remained individualized and stable (for at least 1 year at 4 °C in 150 mM NaCl). On the contrary for PEG_{16}−lipid, no conditions provided satisfactory stabilization. At last, the PEG_{45}−lipid exhibited an intermediate behavior with considerable influence of the initial molar percentage used (the correspondence between the latter and the real molar percentage coated onto particles is presented in the fourth line of Table 4). In conclusion, the discovered general trend was that the higher colloidal stability was obtained with higher PEG molar percentages. This was in good agreement with transition layer evolution measured by SAXS (Table 5) and discussed above.

Conclusions

LipoParticles are organized macromolecular assemblies constituted of a polymer core and a lipid shell. As in the liposome case, they exhibit rather poor colloidal stability in media with relatively high ionic strengths (e.g., 150 mM NaCl). One well-known way to improve liposome colloidal stability by steric repulsions between assemblies is to tether PEG chains on their surfaces. By similitude, PEG chains were added on LipoParticle surfaces by incorporating PEG_n−lipid conjugates in the lipid (DPPC/DPTAP) formulation of vesicles. With the aim of knowing the optimum conditions to reach the colloidal stability of the resulting LipoParticles, a systematic study was carried out as a function of PEG degree of polymerization (*n*) and PEG_n−lipid molar percentage in the lipid formulation. First, we investigated the physicochemical characteristics of the PEG-modified lipid layers surrounding particles. As shown by NMR data, one lipid bilayer around particles was obtained in water, whatever the formulation used. The amount of PEG_n−lipids adsorbed on the polymer particles was found to be impacted by *n* and the PEG_n−lipid molar percentage in the initial lipid formulation. This amount, remaining less than 30%, decreased when *n* increased, probably because of steric hindrance induced by the longest PEG chains. For similar reasons, this amount also decreased with an increase in initial PEG_n−lipid molar percentage, leading to an adsorption plateau limited at 3% with regard to total lipids (with PEG_{45}−lipids). The accurate location of PEG_n−lipids in the inner or outer monolayer of LipoParticle lipid bilayers was assessed by ^{1}H NMR spectroscopy. It was shown that the outer monolayer became the preferential layer

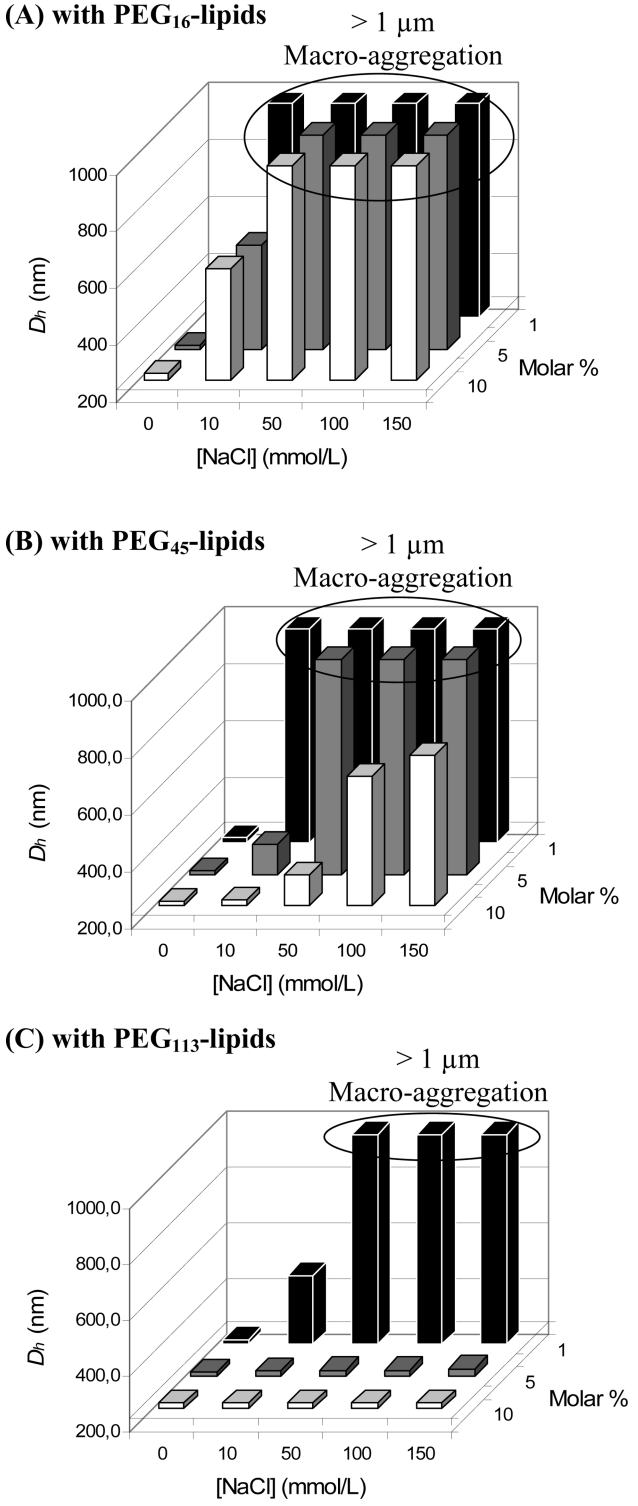

Figure 8. Influence of both molar percentage of PEG_n−lipid in the initial lipid formulation and ionic strength (i.e., NaCl concentration) on the LipoParticle mean hydrodynamic diameter, D_h (1 h at 25 °C): (A) with PEG_{16}−lipid, (B) with PEG_{45}−lipid, (C) with PEG_{113}−lipid. The floors (*xy* plane) correspond to the hydrodynamic diameters of bare PLA particles.

with increases in *n*. Indeed, for $n = 16$, the external and internal layers were equivalent in PEG_n−lipid amounts. For $n = 113$, 90% of PEG_{113}−lipids were located in the outer monolayer as a result of steric hindrance; the bulkier the lipid head, the more difficult the adsorption. The thickness of the lipid layer adsorbed onto PLA particles was determined by SAXS. This thickness was logically found to increase with the PEG chain length (or

with the amount of PEG-lipids really adsorbed). This was explained by taking into account conformation changes (i.e., from mushroom-like to brush-like).

Then, the colloidal stability of PEG-modified LipoParticles was studied by QELS as a function of ionic strength. Clearly, the PEG_{16} shell was not sufficient to induce an efficient steric stabilization. The PEG_{45} shell had an intermediate behavior whereas the PEG_{113} shell provided the best colloidal stability for the resulting LipoParticles. The structural characteristics of the latter were interestingly not affected by relatively high ionic strength (i.e., 150 mM NaCl). The best results obtained with PEG_{113}−lipids were explained by a brush-like conformation of the long PEG chains, whereas for the PEG_{45} shell the PEG chains adopted a mushroom-like conformation. These conformation predictions were based on calculations of the distance between PEG chain grafting points and from the literature about PEG−liposomes. These distance calculations also allowed us to assess the coating thickness. This assessment was found to be similar to the one measured by SAXS. Finally, the critical ionic strength value from which assemblies were aggregated increased with n and the molar percentage of PEG_n−lipids in the lipid formulation.

Acknowledgment. The authors thank Dr. Fernande Boisson (FR2151/CNRS, Vernaison, France) for fruitful discussions about NMR analyses and Dr. Cyrille Rochas (UMR5588/CNRS, St. Martin d'Hères, France) for the experiments at the European Synchrotron Radiation Facility.

References and Notes

(1) Troutier, A.-L.; Ladavière, C. *Adv. Colloid Interface Sci.* **2007**, *133* (1), 1−21.
(2) Eschwege, V.; Laude, I.; Toti, F.; Pasquali, J. L.; Freyssinet, J. M. *Clin. Exp. Immunol.* **1996**, *103* (1), 171−175.
(3) Loidl-Stahlhofen, A.; Eckert, A.; Hartmann, T.; Schottner, M. *J. Pharm. Sci.* **2001**, *90* (5), 599−606.
(4) Bayerl, T.; Bayerl, S. U. S. Patent 5,670,631, 1997.
(5) Bucak, S.; Jones, D. A.; Laibinis, P. E.; Hatton, T. A. *Biotechnol. Prog.* **2003**, *19* (2), 477−484.
(6) Zollner, T. C. A.; Zollner, R. D.; De Cuyper, M.; Santana, M. H. A. *J. Dispersion Sci. Technol.* **2003**, *24* (3−4), 615−622.
(7) Bulte, J. W. M.; De Cuyper, M. Magnetoliposomes as contrast agents. In *Liposomes, Part C*; Duzgunes, N., Ed.; Methods in Enzymology 373; Academic Press: San Diego, CA, 2003; pp 175−198.
(8) von Hoegen, P. *Adv. Drug Delivery Rev.* **2001**, *51* (1−3), 113−125.
(9) El Mir, S.; Casanova, A.; Betbeder, D.; Triebel, F. *Eur. J. Cancer* **2001**, *37* (8), 1053−1060.
(10) Betbeder, D.; Sperandio, S.; Latapie, J. P.; de Nadai, J.; Etienne, A.; Zajac, J. M.; Frances, B. *Pharm. Res.* **2000**, *17* (6), 743−748.
(11) Berton, M.; Sixou, S.; Kravtzoff, R.; Dartigues, C.; Imbertie, L.; Allal, C.; Favre, G. *Biochim. Biophys. Acta-* **1997**, *1355* (1), 7−19.
(12) Debin, A.; Kravtzoff, R.; Santiago, J. V.; Cazales, L.; Sperandio, S.; Melber, K.; Janowicz, Z.; Betbeder, D.; Moynier, M. *Vaccine* **2002**, *20* (21−22), 2752−2763.
(13) Troutier, A.-L.; Delair, T.; Pichot, C.; Ladavière, C. *Langmuir* **2005**, *21* (4), 1305−1313.
(14) Troutier, A.-L.; Véron, L.; Delair, T.; Pichot, C.; Ladavière, C. *Langmuir* **2005**, *21* (22), 9901−9910.
(15) Woodle, M. C. *Adv. Drug Delivery Rev.* **1998**, *32* (1−2), 139−152.
(16) Uster, P. S.; Working, P. K.; Vaage, J. *Int. J. Pharm.* **1998**, *162*, (1−2), 77−86.
(17) Working, P. K.; Newman, M. S.; Sullivan, T.; Yarrington, J. *J. Pharmacol. Exp. Ther.* **1999**, *289* (2), 1128−1133.
(18) Zamboni, W. C.; Gervais, A. C.; Egorin, M. J.; Schellens, J. H. M.; Zuhowski, E. G.; Pluim, D.; Joseph, E.; Hamburger, D. R.; Working, P. K.; Colbern, G.; Tonda, M. E.; Potter, D. M.; Eiseman, J. L. *Cancer Chemother. Pharmacol.* **2004**, *53* (4), 329−336.
(19) Working, P. K.; Newman, M. S.; Sullivan, T.; Brunner, M.; Podell, M.; Sahenk, Z.; Turner, N. *Toxicol. Sci.* **1998**, *46* (1), 155−165.
(20) Lukyanov, A. N.; Elbayoumi, T. A.; Chakilam, A. R.; Torchilin, V. P. *J. Controlled Release* **2004**, *100* (1), 135−144.
(21) Steenpa*β*, T.; Lung, A.; Schubert, R. *Biochim. Biophys. Acta* **2006**, *1758* (1), 20−28.
(22) Meyer, O.; Kirpotin, D.; Hong, K.; Sternberg, B.; Park, J. W.; Woodle, M. C.; Papahadjopoulos, D. *J. Biol. Chem.* **1998**, *273* (26), 15621−15627.
(23) Frisch, B.; Carrière, M.; Largeau, C.; Mathey, F.; Masson, C.; Schuber, F.; Scherman, D.; Escriou, V. *Bioconjugate Chem.* **2004**, *15* (4), 754−764.
(24) Önyüksel, H.; Séjourné, F.; Suzuki, H.; Rubinstein, I. *Peptides* **2006**, *27* (9), 2271−2275.
(25) Woodle, M. C.; Storm, G.; Newman, M. S.; Jekot, J. J.; Collins, L. R.; Martin, F. J.; Francis, C.; Szoka, J. *Pharm. Res.* **1992**, *9* (2), 260−265.
(26) Kim, A.; Yun, M.-O.; Oh, Y.-K.; Ahn, W.-S.; Kim, C.-K. *Int. J. Pharm.* **1999**, *180* (1), 75−81.
(27) Singh, S. K.; Bisen, P. S. *Vaccine* **2006**, *24* (19), 4161−4166.
(28) Awasthi, V. D.; Garcia, D.; Klipper, R.; Goins, B. A.; Phillips, W. T. *J. Pharmacol. Exp. Ther.* **2004**, *309* (1), 241−248.
(29) Oku, N. *Adv. Drug Delivery Rev.* **1999**, *37* (1−3), 53−61.
(30) Dos Santos, N.; Allen, C.; Doppen, A.-M.; Anantha, M.; Cox, K. A. K.; Gallagher, R. C.; Karlsson, G.; Edwards, K.; Kenner, G.; Samuels, L.; Webb, M. S.; Bally, M. B. *Biochim. Biophys. Acta* **2007**, *1768* (6), 1367−1377
(31) Sears, B. D. Synthetic Phospholipid Compounds. U. S. Patent 4,-426,330, 1984.
(32) Fessi, H.; Devissaguet, J.-P.; Puisieux, F.; Thies, C. Preparation process for disperse colloidal systems from a substance in the shape of nanoparticles. EP Patent 0,275,796, 1988.
(33) Lasic, D. D. *Liposomes: From Physics to Applications*; Elsevier: Amsterdam, 1993; pp 63−107.
(34) Silvius, J. R. *Biochim. Biophys. Acta* **1991**, *1070* (1), 51−59.
(35) Takayama, M.; Itoh, S.; Nagasaki, T.; Tanimizu, I. *Clin. Chim. Acta* **1977**, *79* (1), 93.
(36) Koppel, D. E. *J. Chem. Phys.* **1972**, *57* (11), 4814−4820.
(37) Coombes, A. G. A.; Scholes, P. D.; Davies, M. C.; Illum, L.; Davis, S. S. *Biomaterials* **1994**, *15* (9), 673.
(38) Hunter, R. J. *Zeta Potential in Colloid Science: Principles and Applications*; Colloid Science 2; Academic Press: London, 1981.
(39) Vernooij, E. A. A. M.; Gentry, C. A.; Herron, J. N.; Crommelin, D. J. A.; Kettenes-van den Bosch, J. J. *Pharm. Res.* **1999**, *16* (10), 1658−1661.
(40) Garcia-Fuentes, M.; Torres, D.; Martin-Pastor, M.; Alonso, M. J. *Langmuir* **2004**, *20* (20), 8839−8845.
(41) Nagle, J. F.; Tristram-Nagle, S. *Biochim. Biophys. Acta* **2000**, *1469* (3), 159−195.
(42) Vauthier, C.; Schmidt, C.; Couvreur, P. *J. Nanopart. Res.* **1999**, *1* (3), 411−418.
(43) Kim, M.-H. *J. Appl. Crystallogr.* **2004**, *37* (4), 643−651.
(44) Tirosh, O.; Barenholz, Y.; Katzhendler, J.; Priev, A. *Biophys. J.* **1998**, *74* (3), 1371−1379.
(45) Mornet, S.; Lambert, O.; Duguet, E.; Brisson, A. *Nano Lett.* **2005**, *5* (2), 281−285.
(46) De Cuyper, M.; Muller, P.; Lueken, H.; Hodenius, M. *J. Phys.: Condens. Matter* **2003**, *15* (15), S1425−S1436.
(47) De Cuyper, M.; Valtonen, S. *J. Magn. Magn. Mater.* **2001**, *225* (1−2), 89−94.
(48) De Cuyper, M.; Hodenius, M.; Lacava, Z. G. M.; Azevedo, R. B.; da Silva, M. D.; Morais, P. C.; Santana, M. H. A. *J. Colloid Interface Sci.* **2002**, *245* (2), 274−280.
(49) Hodenius, M.; De Cuyper, M.; Desender, L.; Muller-Schulte, D.; Steigel, A.; Lueken, H. *Chem. Phys. Lipids* **2002**, *120* (1−2), 75−85.
(50) De Cuyper, M.; Crabbe, A.; Cocquyt, J.; Van der Meeren, P.; Martins, F.; Santana, M. H. A. *Phys. Chem. Chem. Phys.* **2004**, *6* (7), 1487−1492.
(51) Garbuzenko, O.; Barenholz, Y.; Priev, A. *Chem. Phys. Lipids* **2005**, *135* (2), 117−129.
(52) Kenworthy, A. K.; Hristova, K.; Needham, D.; McIntosh, T. J. *Biophys. J.* **1995**, *68* (5), 1921−1936.
(53) de Gennes, P. G. *Adv. Colloid Interface Sci.* **1987**, *27* (3−4), 189−209.
(54) Lasic, D. D.; Papahadjopoulos, D. *Curr. Opin. Solid State Mater. Sci.* **1998**, *1* (3), 392−400.
(55) Hristova, K.; Needham, D. *J. Colloid Interface Sci.* **1994**, *168* (2), 302−314.

BM700753Q